

Tetranuclear Ni^{II} and Dinuclear Mn^{III} Complexes Derived from a New Macrocyclic Ligand with Four Endogenous Phenolic Groups

Kazuhide Ikeda, Kanako Matsufuji, Masaaki Ohba,* Masahito Kodera,¹ and Hisashi Ōkawa*

Department of Chemistry, Faculty of Science, Kyushu University,
Hakozaki 6-10-1, Higashiku, Fukuoka 812-8581

¹Department of Molecular Science and Technology, Doshisha University,
Kyotanabe, Kyoto 610-0321

Received August 25, 2003; E-mail: okawascc@mbx.nc.kyushu-u.ac.jp

A tetranucleating macrocyclic ligand with four endogenous phenolic groups is obtained by the condensation of 3-aminomethyl-5-methylsalicylaldehyde in the presence of metal ion as two tetranuclear Ni^{II} complexes, [Ni₄(L)(OH)(H₂O)₄](ClO₄)₃ (**1**) and [Ni₄(L)(O)(dmf)₄](ClO₄)₂ (**2**), and a dinuclear Mn^{III} complex, [Mn₂(H₂L)(OH)(AcO)₂(H₂O)]Br (**3**). X-ray crystallographic studies for [Ni₄(L)(OH)(H₂O)₈](ClO₄)₃·7H₂O (**1'**) indicate that the macrocyclic ligand accommodates four Ni^{II} ions, producing a square Ni₄ core with μ₄-hydroxo group at the center of the core. Water molecules occupy the axial sites of each Ni affording a nearly octahedral geometry about the metal. Complex **2** has a similar tetranuclear Ni₄-core possessing a μ₄-oxo group at the center of the core. In complex **3**, the di-protonated ligand (H₂L)²⁺ accommodates two Mn^{III} ions, affording a (μ-hydroxo)(μ-acetato)dimanganese(III) core. Magnetic studies for **1** and **2** indicate a ferromagnetic interaction between the adjacent Ni^{II} centers and an antiferromagnetic interaction between the diagonal Ni^{II} centers. Complex **3** shows a weak antiferromagnetic interaction between the two Mn^{III} ions.

Polynuclear metal complexes are of interest in physicochemical properties and functions arising from an interaction or interplay of metal ions in close proximity. Recent attention has been directed to the organization of three or more metal ions in a predetermined array using macrocyclic compartmental ligands. For example, tetranuclear Ni(II) and Zn(II) complexes and hexanuclear Cu(II) complexes have been obtained using the [2 + 2] and [3 + 3] condensation products between 2,6-diformyl-4-methylphenol and 2,6-bis(aminomethyl)-4-methylphenol (A and B, respectively, of Fig. 1)^{1,2} and tetra-, octa-, and dodecanuclear metal complexes have been prepared using the [2 + 2] condensation product between 2,6-diformyl-4-methylphenol and 1,5-diamino-3-pentanol (Fig. 1, C).^{3–6} We have recently developed a tetranucleating compartmental ligand having two N(amine)₂O₂ and two N(imine)₂O₂ metal-binding sites that share two phenolic oxygen atoms in the alternative fashion in the macrocyclic framework (Fig. 1, D).^{7,8} The ligand shows a site specificity of metal ions affording mixed-metal M^{II}₂Cu^{II}₂ complexes of a deficient double-cubane structure (M = Ni) or a dimer-of-dimers structure (M = Co, Zn).

This work relates to metal complexes of a new macrocyclic ligand (abbreviated as L⁴⁺, see Fig. 2) derived from the cyclic condensation of four molecules of 3-aminomethyl-5-methylsalicylaldehyde in the presence of a metal ion. Two tetranuclear Ni^{II} complexes, [Ni₄(L)(OH)(H₂O)₄](ClO₄)₃ (**1**) and [Ni₄(L)(O)(dmf)₄](ClO₄)₂ (**2**), have been derived by the condensation of 3-aminomethyl-5-methylsalicylaldehyde in the presence of Ni^{II} ion. Furthermore, dinuclear [Mn₂(H₂L)(OH)(AcO)₂(H₂O)]Br (**3**) has been produced by a similar condensation in the presence of Mn^{II} in open air. Their structures and physicochemical properties are reported.

Experimental

Physical Measurements. Elemental analyses of carbon, hydrogen, and nitrogen were obtained at The Service Center of Elemental Analysis of Kyushu University. Infrared spectra were measured using a KBr disk on a PERKIN ELEMER Spectrum BX FT-IR system. Fast atom bombardment (FAB) mass spectra were recorded on a JMS-SX/SX102A Tandem mass spectrometer using *m*-nitrobenzylalcohol as the matrix. Electronic spectra in acetonitrile were recorded on a Shimadzu UV-3100PC spectrophotometer. Magnetic susceptibilities were measured on a Quantum Design MPMS2 XL SQUID susceptometer in the temperature range of 2–300 K.

Preparation. 3-Aminomethyl-5-methylsalicylaldehyde Hydrobromide: A solution of 3-chloromethyl-5-methylsalicylaldehyde⁹ (10 g, 0.054 mol), potassium phthalimide (20 g, 0.108 mol) in *N,N*-dimethylformamide (80 cm³) was heated at 90 °C for 12 h. The reaction mixture was evaporated to dryness and the residue was thoroughly washed with water. Crystallization from a dichloromethane/ethanol mixture (1:1 in volume) gave 3-phthalimidomethyl-5-methylsalicylaldehyde as yellow needles. The yield was 6.91 g (43%).

A mixture of 48% hydrobromic acid (50 cm³), glacial acetic acid (50 cm³) and 3-phthalimidomethyl-5-methylsalicylaldehyde (5.0 g, 0.017 mol) was heated under reflux for 3 days and allowed to stand over night. The resulting phthalic acid was separated by filtration and the filtrate was evaporated to dryness to give a brown precipitate. It was thoroughly washed with dichloromethane and crystallized from ethanol as pale yellow needles. The yield was 2.93 g (71%). Anal. Found: C, 43.58; H, 4.97; N, 5.89%. Calcd for C₉H₁₂BrNO₂: C, 43.92; H, 4.91; N, 5.69%. Selected IR data [ν/cm⁻¹] on KBr disk: 3000 (br), 1645, 1607, 1482, 1470, 1377,

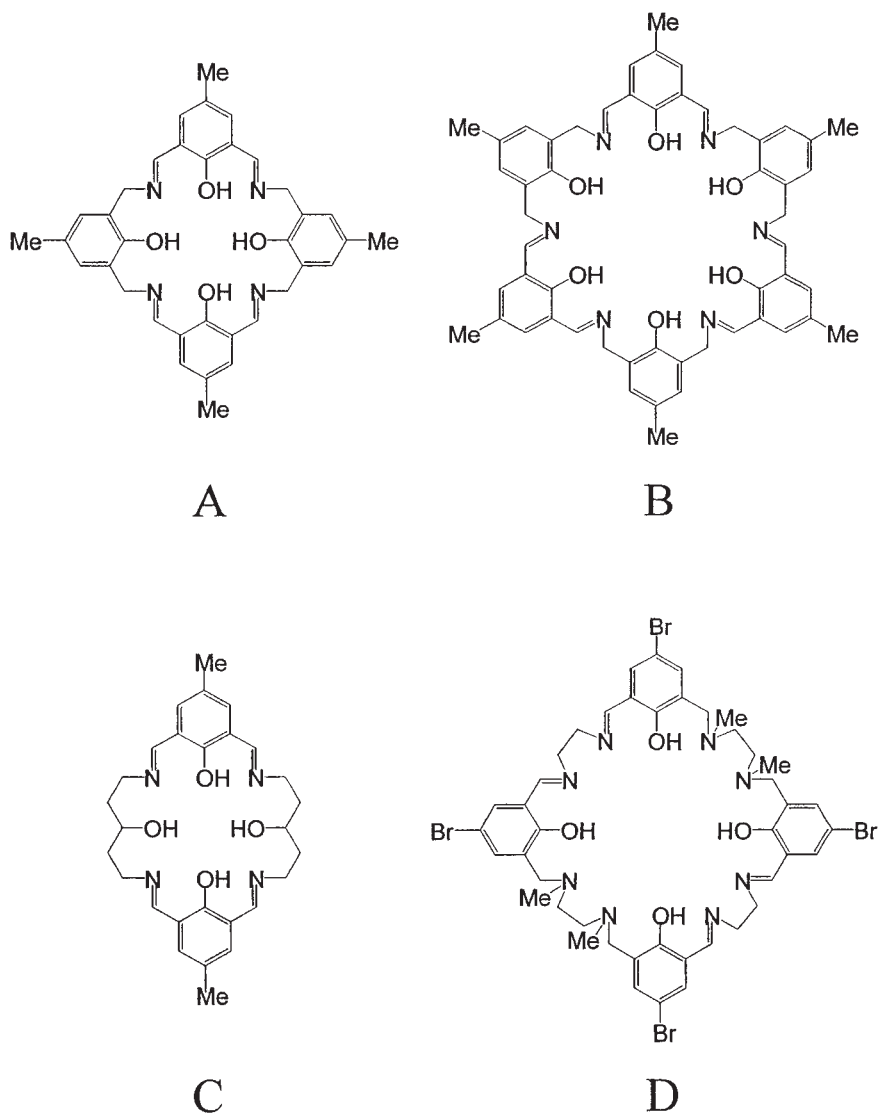
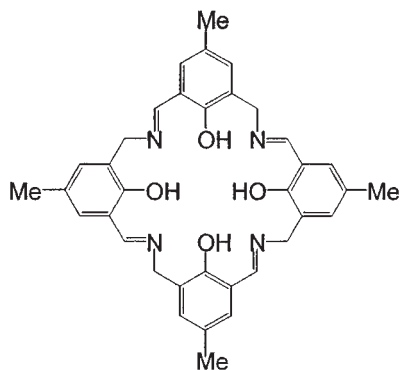


Fig. 1. Chemical structures of polynucleating macrocyclic ligands.

Fig. 2. Chemical structure of H_4L .

1309, 1265, 1124, 1080, 713.

$[\text{Ni}_4(\text{L})(\text{OH})(\text{H}_2\text{O})_4](\text{ClO}_4)_3$ (1): 3-Aminomethyl-5-methylsalicylaldehyde hydrobromide (123 mg, 0.5 mmol), nickel perchlorate hexahydrate (365 mg, 1 mmol) and sodium perchlorate (245 mg, 2 mmol) were dissolved in methanol (17 cm^3). To this was added a solution of potassium hydroxide (56 mg, 1 mmol)

in methanol (7 cm^3), and the mixture was heated under reflux for 2 h. The reaction mixture was diluted with 40 cm^3 of water and then the volume of the solution was reduced to ca. 20 cm^3 by vacuum distillation. This was allowed to stand for a few days to form efflorescent green crystals of $[\text{Ni}_4(\text{L})(\text{OH})(\text{H}_2\text{O})_8](\text{ClO}_4)_3 \cdot 7\text{H}_2\text{O}$ (**1'**). The yield was 53 mg (33%). Analytical data were obtained for a sample dehydrated at 80 $^\circ\text{C}$ in vacuo and the results agreed with the formula of $[\text{Ni}_4(\text{L})(\text{OH})(\text{H}_2\text{O})_4](\text{ClO}_4)_3$. Anal. Found: C, 35.59; H, 3.48; N, 4.56%. Calcd for $\text{C}_{36}\text{H}_{41}\text{Cl}_3\text{N}_4\text{Ni}_4\text{O}_{21}$: C, 35.82; H, 3.42; N, 4.64%. Selected IR data [ν/cm^{-1}] on KBr disk: 3438, 2916, 1646, 1566, 1460, 1398, 1294, 1269, 1110, 1091, 817, 627. UV-vis [λ/nm ($\epsilon/\text{M}^{-1}\text{cm}^{-1}$)]: 355 (14000), 618 (81), 850 (59) in acetonitrile. FAB-mass [m/z]: 1035 for $\{\text{Ni}_4(\text{L})(\text{OH})(\text{ClO}_4)_2\}^+$.

$[\text{Ni}_4(\text{L})(\text{O})(\text{dmf})_4](\text{ClO}_4)_2$ (2): Complex **1** was dissolved in DMF and the solution was diffused with ether to result in the precipitation of green crystals. The yield was ca. 70%. Anal. Found: C, 43.44; H, 4.91; N, 8.36%. Calcd for $\text{C}_{48}\text{H}_{60}\text{Cl}_2\text{N}_8\text{Ni}_4\text{O}_{17}$: C, 43.45; H, 4.56; N, 8.45%. Selected IR data [ν/cm^{-1}] on KBr disk: 3340, 2924, 1650, 1646, 1561, 1459, 1301, 1109, 1091, 816, 626. UV-vis [λ/nm ($\epsilon/\text{M}^{-1}\text{cm}^{-1}$)]: 360 (15000), 620 (90), 910 (76) in

acetonitrile. FAB-mass [m/z]: 933 for $\{\text{Ni}_4(\text{L})(\text{O})(\text{ClO}_4)\}^+$.

[Mn₂(H₂L)(OH)(AcO)₂(H₂O)]Br (3): Manganese(II) acetate tetrahydrate (268 mg, 1 mmol) and 3-aminomethyl-5-methylsalicylaldehyde hydrobromide (246 mg, 1 mmol) were dissolved in methanol (15 cm³). To this were successively added a solution of triethylamine (202 mg, 2 mmol) in methanol (5 cm³) and a solution of sodium acetate (160 mg, 2 mmol) in methanol (10 cm³); this mixture was heated under reflux for 6 h. The resulting dark-brown solution was reduced to 10 cm³ and diluted with 40 cm³ of water. After a few days, dark brown crystals of $[\text{Mn}_2(\text{H}_2\text{L})(\text{OH})(\text{AcO})_2(\text{H}_2\text{O})]\text{Br}$ (**3**) separated out. The yield was 60 mg (26%). Anal. Found: C, 52.10; H, 4.57; N, 6.10%. Calcd for $\text{C}_{40}\text{H}_{43}\text{BrMn}_2\text{N}_4\text{O}_{10}$: C, 51.71; H, 4.67; N, 6.03%. Selected IR data [ν/cm^{-1}] on KBr disk: 3392 (br), 1658, 1624, 1563, 1557, 1473, 1456, 1424, 1312, 1265, 1211, 1047, 835, 590. UV-vis [λ/nm ($\epsilon/\text{M}^{-1}\text{cm}^{-1}$)]: 360 (14600) in acetonitrile.

Crystal Structure Analyses. A single crystal of $[\text{Ni}_4(\text{L})(\text{OH})(\text{H}_2\text{O})_8](\text{ClO}_4)_3 \cdot 7\text{H}_2\text{O}$ (**1'**) was mounted on a glass fiber and coated with epoxy resin. Measurements were carried out on a Rigaku/MSC Mercury diffractometer with graphite monochromated Mo K α radiation. The data were collected at $-90 \pm 1^\circ\text{C}$ to a maximum 2θ value of 55.0° . A total of 1240 oscillation images were collected. The exposure rate was $33.3\text{ sec}/^\circ$, the detector sweep angle was 19.7° and the crystal-to-detector distance was 45.05 mm. The linear absorption coefficient, μ , for Mo K α radiation was 14.9 cm^{-1} . Absorption correction was not applied. The data were corrected for Lorentz and polarization effects. Pertinent crystallographic parameters are summarized in Table 1.

The structures were solved by direct method and expanded using Fourier techniques. The non-hydrogen atoms were refined anisotropically. Hydrogen atoms were included but not refined. The final cycle of full-matrix least-squares refinement was based on 12524 observed reflections ($I > 2.00\sigma(I)$, $2\theta < 54.96$) and 721 variable parameters.

Neutral atom scattering factors were taken from Cromer and Waber.¹⁰ Anomalous dispersion effects were included in F_{calc} ;

Table 1. Crystallographic Parameters for $[\text{Ni}_4(\text{L})(\text{OH})(\text{H}_2\text{O})_8](\text{ClO}_4)_3 \cdot 7\text{H}_2\text{O}$ (**1'**)

Complex	(1')
Formula	$\text{C}_{36}\text{H}_{65}\text{N}_4\text{Cl}_3\text{Ni}_4\text{O}_{33}$
fw	1423.08
Crystal color	green
Crystal size/mm ³	$0.25 \times 0.20 \times 0.05$
$T/^\circ\text{C}$	-90 ± 1
Crystal system	monoclinic
Space group	$P2_1/n$ (#14)
$a/\text{\AA}$	14.268(1)
$b/\text{\AA}$	19.056(1)
$c/\text{\AA}$	20.520(2)
$\beta/^\circ$	92.013(4)
$V/\text{\AA}^3$	5575.563(1)
Z	4
$D_{\text{calc}}/\text{g cm}^{-3}$	1.695
$\mu(\text{Mo K}\alpha)/\text{cm}^{-1}$	15.72
No. of reflections	12524 (all data) 7214 ($I > 2\sigma(I)$)
R	0.109
R_w	0.189
R_1	0.073

the values for $\Delta f'$ and $\Delta f''$ were those of Creagh and McAuley.¹¹ The values for the mass attenuation coefficients are those of Creagh and Hubbel.¹² All calculations were performed using the teXsan¹³ crystallographic software package of Molecular Structure Corporation.

Crystallographic data have been deposited at the CCDC, 12 Union Road, Cambridge CB2 1EZ, UK and copies can be obtained on request, free of charge, by quoting the publication citation and the deposition numbers 212317 and 212318.

Result and Discussion

Preparation and General Properties. The condensation of 3-aminomethyl-5-methylsalicylaldehyde in the presence of Ni^{II} afforded tetranuclear $[\text{Ni}_4(\text{L})(\text{OH})(\text{H}_2\text{O})_4](\text{ClO}_4)_3$ (**1**) and $[\text{Ni}_4(\text{L})(\text{O})(\text{dmf})_4](\text{ClO}_4)_2$ (**2**). The μ_4 -hydroxo complex **1** was obtained by crystallization from an aqueous solution, and the μ_4 -oxo complex **2** was obtained when **1** was crystallized from DMF. We confirmed that **2** was converted into **1** when a suspension of **2** in a dilute perchloric acid was stirred at room temperature. This fact suggests that **1** and **2** have a similar tetranuclear core. FAB mass spectrometric studies for **1** indicate a parent ion peak at $m/z = 1035$ that corresponds to $\{\text{Ni}_4(\text{L})(\text{OH})(\text{ClO}_4)_2\}^+$. Complex **2** shows an ion peak at $m/z = 933$ corresponding to $\{\text{Ni}_4(\text{L})(\text{O})(\text{ClO}_4)\}^+$.

The electronic absorption spectrum of **1** in acetonitrile has three bands at 355, 618, and 850 nm. The intense band at 355 nm is assigned to the π - π^* transition associated with the azomethine group.^{14,15} The absorption bands at 618 and 850 nm can be assigned to d-d transitions of the Ni^{II} in an octahedral geometry. The absorption spectrum of **2** in acetonitrile resembles that of **1** and shows three bands at 360, 620, and 910 nm.

The condensation of 3-aminomethyl-5-methylsalicylaldehyde in the presence of Mn^{II} in open air gave dinuclear $[\text{Mn}_2(\text{H}_2\text{L})(\text{OH})(\text{AcO})_2]\text{Br} \cdot \text{H}_2\text{O}$ (**3**). The IR bands at 1561 and 1419 cm^{-1} can be assigned to the $\nu_{\text{as}}(\text{COO})$ and $\nu_{\text{s}}(\text{COO})$ vibrations of acetate group, respectively. The small separation between the two bands ($<150\text{ cm}^{-1}$) suggests the presence of a bridging acetate group in the molecule.¹⁶ The absorption spectrum of **3** shows an intense azomethine π - π^* band at 390 nm. The d-d bands due to Mn^{III} are not well resolved.

Crystal Structures. $[\text{Ni}_4(\text{L})(\text{OH})(\text{H}_2\text{O})_8](\text{ClO}_4)_3 \cdot 7\text{H}_2\text{O}$ (**1'**): The crystallographic results for **1'** are not complete enough, due to the efflorescent nature of the crystal, but they clearly demonstrate the unique tetranuclear core of the complex. ORTEP¹⁷ views are given in Fig. 3 together with the atom numbering scheme. Selected bond distances and angles are summarized in Table 2.

The asymmetric unit consists of one $[\text{Ni}_4(\text{L})(\text{OH})(\text{H}_2\text{O})_8]^{3+}$ cation, three perchlorate ions and seven lattice water molecules. The cation has four Ni atoms in a square arrangement and has a μ_4 -hydroxo group at the center of the square core. Each Ni^{II} is bonded to the {ONO} donor set of the macrocyclic ligand and to the exogenous μ_4 -hydroxo oxygen O(5). The Ni-to-macrocycle bond distances range from $1.957(5)\text{ \AA}$ to $2.029(4)\text{ \AA}$. The Ni-to-O(5) bond distance is longer ($2.144(4)$ – $2.163(4)\text{ \AA}$). The hydroxide oxygen O(5) is $0.300(4)\text{ \AA}$ displaced from the least-squares plane defined by four nickel atoms, affording a hat-like shape for the complex molecule. Each Ni has a pseu-

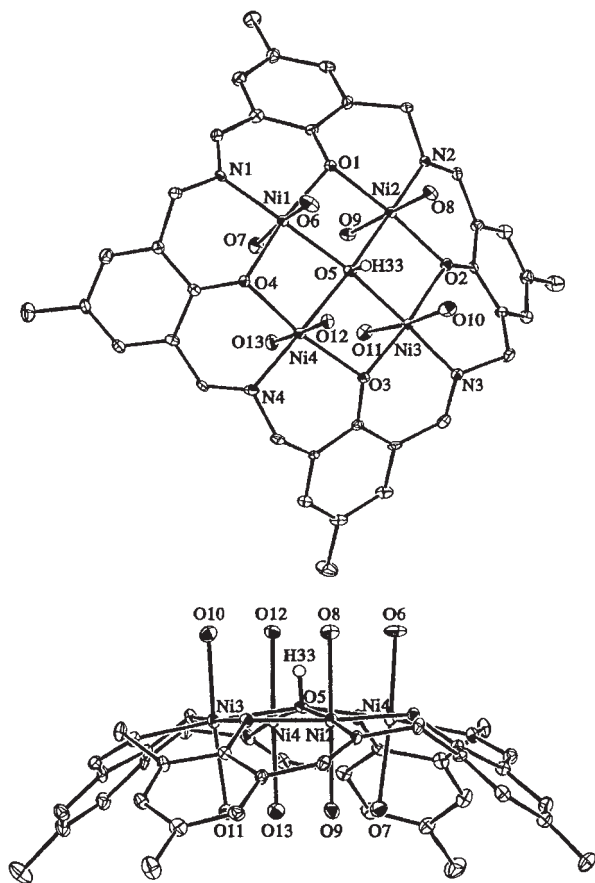


Fig. 3. ORTEP views of $[\text{Ni}_4(\text{L})(\text{OH})(\text{H}_2\text{O})_8](\text{ClO}_4)_3 \cdot 7\text{H}_2\text{O}$ (**1'**) with atom numbering scheme.

do octahedral geometry with water molecules at the axial sites. The Ni–O(water) bond distances on the closed face (2.124(5)–2.128(5) Å) are significantly longer than the Ni–O(water) bond distances on the open face (2.066(5)–2.098(4) Å). It appears that the water molecules on the closed face are released on dehydration affording $[\text{Ni}_4(\text{L})(\text{OH})(\text{H}_2\text{O})_4](\text{ClO}_4)_3$ (**1**). The mean of the adjacent Ni...Ni distances is 3.01 Å and the mean of the diagonal Ni...Ni distances is 4.26 Å.

The related macrocyclic ligand **A** (L_A^{4-}) in Fig. 1 is shown to afford μ_4 -hydroxotetranickel(II) complexes of a $[\text{Ni}_4(\text{L}_A)(\text{OH})(\text{CH}_3\text{O} \cdot \text{H} \cdot \text{OCH}_3)]^{2+}$ core of a bowl structure, where the hydroxide group acts as a μ_4 -bridge at the bottom of the bowl and a pair of nickel ions are bridged by methoxo group (two methoxo groups are hydrogen-bonded through proton). Thus, the tetranuclear Ni core can be regarded as a dimer-of-dimers structure. The bowl structure of the Ni complexes results from the flexibility of L_A^{4-} , owing to the localization of C=N bonds in the macrocyclic framework. Obviously, the macrocyclic ligand L^{4-} is less flexible than L_A^{4-} due to the symmetric arrangement of C=N bonds in the macrocyclic framework.

[Mn₂(H₂L)(OH)(AcO)₂(H₂O)]Br (3**):** The structure of **3** could not be fully solved due to the poor quality of the crystal.¹⁸ The macrocyclic ligand protonated at two imine nitrogen atoms, $(\text{H}_2\text{L})^{2-}$, accommodates two Mn^{III} ions using two ONO-donor sets (see Fig. 4). The pair of Mn ions are doubly bridged by hydroxide and acetate groups. One acetate group

Table 2. Selected Bond Distances (Å) and Angles (°) for $[\text{Ni}_4(\text{L})(\text{OH})(\text{H}_2\text{O})_8](\text{ClO}_4)_3 \cdot 7\text{H}_2\text{O}$ (**1'**)

Bond distances/Å			
Ni(1)–O(1)	2.019(4)	Ni(3)–O(2)	2.022(4)
Ni(1)–O(4)	2.020(4)	Ni(3)–O(3)	2.007(4)
Ni(1)–O(5)	2.145(4)	Ni(3)–O(5)	2.147(4)
Ni(1)–O(6)	2.087(5)	Ni(3)–O(10)	2.082(5)
Ni(1)–O(7)	2.139(5)	Ni(3)–O(11)	2.140(5)
Ni(1)–N(1)	1.967(5)	Ni(3)–N(3)	1.959(5)
Ni(2)–O(1)	2.029(4)	Ni(4)–O(3)	2.020(4)
Ni(2)–O(2)	1.992(4)	Ni(4)–O(4)	1.995(4)
Ni(2)–O(5)	2.166(4)	Ni(4)–O(5)	2.149(4)
Ni(2)–O(8)	2.101(4)	Ni(4)–O(12)	2.096(4)
Ni(2)–O(9)	2.132(5)	Ni(4)–O(13)	2.137(4)
Ni(2)–N(2)	1.970(5)	Ni(4)–N(4)	1.968(5)
Angles/deg			
O(1)–Ni(1)–O(4)	172.0(2)	O(2)–Ni(3)–O(3)	172.7(2)
O(1)–Ni(1)–O(5)	86.1(2)	O(2)–Ni(3)–O(5)	87.1(2)
O(1)–Ni(1)–O(6)	91.1(2)	O(2)–Ni(3)–O(10)	86.9(2)
O(1)–Ni(1)–O(7)	93.0(2)	O(2)–Ni(3)–O(11)	89.2(2)
O(1)–Ni(1)–N(1)	92.7(2)	O(2)–Ni(3)–N(3)	94.1(2)
O(4)–Ni(1)–O(5)	86.3(2)	O(3)–Ni(3)–O(5)	85.9(2)
O(4)–Ni(1)–O(6)	86.0(2)	O(3)–Ni(3)–O(10)	90.5(2)
O(4)–Ni(1)–O(7)	89.5(2)	O(3)–Ni(3)–O(11)	92.9(2)
O(4)–Ni(1)–N(1)	95.0(2)	O(3)–Ni(3)–N(3)	93.1(2)
O(5)–Ni(1)–O(6)	86.6(2)	O(5)–Ni(3)–O(10)	85.5(2)
O(5)–Ni(1)–O(7)	90.2(2)	O(5)–Ni(3)–O(11)	90.7(2)
O(5)–Ni(1)–N(1)	175.1(2)	O(5)–Ni(3)–N(3)	176.2(2)
O(6)–Ni(1)–O(7)	174.6(2)	O(10)–Ni(3)–O(11)	174.7(2)
O(6)–Ni(1)–N(1)	98.2(2)	O(10)–Ni(3)–N(3)	98.2(2)
O(7)–Ni(1)–N(1)	85.1(2)	O(11)–Ni(3)–N(3)	85.7(2)
O(1)–Ni(2)–O(2)	172.2(2)	O(3)–Ni(4)–O(4)	171.7(2)
O(1)–Ni(2)–O(5)	85.3(2)	O(3)–Ni(4)–O(5)	85.5(2)
O(1)–Ni(2)–O(8)	89.4(2)	O(3)–Ni(4)–O(12)	89.9(2)
O(1)–Ni(2)–O(9)	90.3(2)	O(3)–Ni(4)–O(13)	91.4(2)
O(1)–Ni(2)–N(2)	95.5(2)	O(3)–Ni(4)–N(4)	95.7(2)
O(2)–Ni(2)–O(5)	87.3(2)	O(4)–Ni(4)–O(5)	86.8(2)
O(2)–Ni(2)–O(8)	87.8(2)	O(4)–Ni(4)–O(12)	86.6(2)
O(2)–Ni(2)–O(9)	92.2(2)	O(4)–Ni(4)–O(13)	92.0(2)
O(2)–Ni(2)–N(2)	92.0(2)	O(4)–Ni(4)–N(4)	92.1(2)
O(5)–Ni(2)–O(8)	87.3(1)	O(5)–Ni(4)–O(12)	87.4(2)
O(5)–Ni(2)–O(9)	90.0(1)	O(5)–Ni(4)–O(13)	91.6(2)
O(5)–Ni(2)–N(2)	176.0(2)	O(5)–Ni(4)–N(4)	176.4(2)
O(8)–Ni(2)–O(9)	177.4(2)	O(12)–Ni(4)–O(13)	178.3(2)
O(8)–Ni(2)–N(2)	96.6(2)	O(12)–Ni(4)–N(4)	96.0(2)
O(9)–Ni(2)–N(2)	86.1(2)	O(13)–Ni(4)–N(4)	85.0(2)

unidentately coordinates to one Mn and one water molecule coordinates to another Mn affording a six-coordinate geometry for both Mn centers.

The crystallographic study for **1** demonstrates that the ligand $(\text{L})^{4-}$ has a cavity suitable for accommodating four Ni^{II} ions (ionic radius: 0.84 Å¹⁸) producing a square Ni₄ core with a μ_4 -hydroxo or μ_4 -oxo bridge at the center of the core. Such a tetranuclear square core must be difficult to produce with smaller Mn^{III} ions (ionic radius: 0.79 Å¹⁹). The μ -hydroxo- μ -carboxylato-dimanganese(III) core found for **2** is rather rare though μ -oxo-di(μ -carboxylato)-dimanganese(III) core is commonly known.²⁰

Magnetic Properties. Magnetic properties of **1** and **2** are of

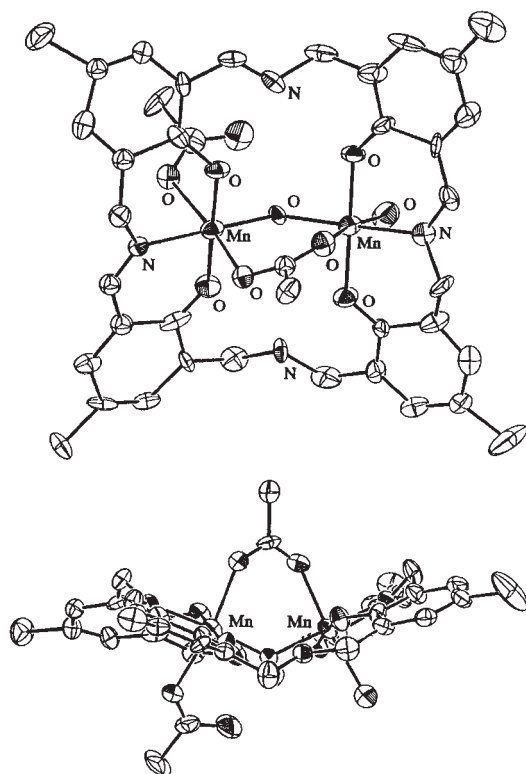


Fig. 4. The structure of $[\text{Mn}_2(\text{H}_2\text{L})(\text{OH})(\text{AcO})_2(\text{H}_2\text{O})]\text{Br}$ (**3**).

interest because of their unique square core structure. Cryo-magnetic properties of **1** and **2** are given in Fig. 5. The effective magnetic moment of **1** (per metal) is $3.04 \mu_B$ at room temperature and the moment decreased with decreasing temperature to $0.62 \mu_B$ at 2 K. The effective magnetic moment of **2** is $2.99 \mu_B$ at room temperature and the moment decreased with decreasing temperature to $0.33 \mu_B$ at 2 K. The results indicate that antiferromagnetic interaction is dominant in each complex molecule.

Using the spin system given in Fig. 6, the spin Hamiltonian based on Heisenberg model ($H = -2\sum J_{ij}S_iS_j$) is expressed by Eq. 1:

$$H = -2J(S_1S_2 + S_2S_3 + S_3S_4 + S_4S_1) - 2J'(S_1S_3 + S_2S_4) \quad (1)$$

where J is the exchange integral between the adjacent Ni centers and J' is the exchange integral between the diagonal Ni centers. The spin states defined by $S_T (= S_{13} + S_{24})$, $S_{13} (= S_1 + S_3)$, and $S_{24} (= S_2 + S_4)$ are determined by Kambe's method and their energies are obtained by Eq. 1. Using the Van Vleck equation, the magnetic susceptibility expression for the system is derived as follows:

$$\chi_A = (1 - \rho)\{Ng^2\beta^2/2k(T - \theta)\}\{A/B\} + \rho\{2Ng^2\beta^2/3kT\} + N\alpha \quad (2)$$

where $A = 30 \exp(8x+12y) + 14 \exp(12y) + 5 \exp(-6x+12y) + \exp(-10x+12y) + 28 \exp(4x+8y) + 10 \exp(-2x+8y) + 2 \exp(-6x+8y) + 10 \exp(6y) + 5 \exp(2x+4y) + \exp(-2x+6y) + 2 \exp(2y)$ and $B = 9 \exp(8x+12y) + 7 \exp(12y) + 5 \exp(-6x+12y) + 3 \exp(-10x+12y) + \exp(-12x+12y) + 14 \exp(4x+8y) + 10 \exp(-2x+8y) + 6 \exp(-6x+8y) + 10 \exp(6y) + 5 \exp(2x+4y) + 3 \exp(-2x+4y) + \exp(-4x+4y) + 6 \exp(2y) + 1$ with $x = J/kT$ and $y = J'/kT$.

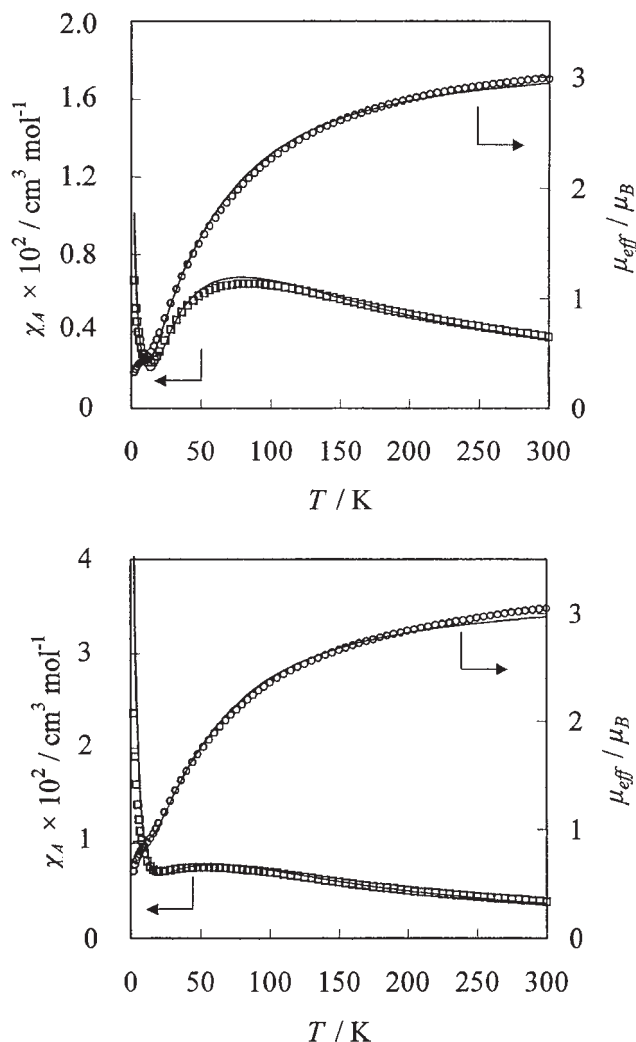


Fig. 5. χ_M vs T and μ_{eff} vs T curves for **1** and **2**.

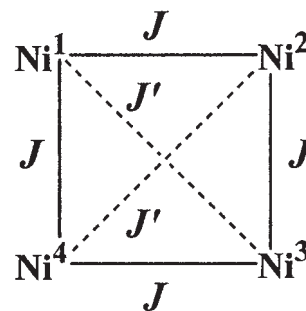


Fig. 6. The spin system for square Ni_4 system.

$4y) + 6 \exp(2y) + 1$ with $x = J/kT$ and $y = J'/kT$.

In this equation, ρ is the fraction of paramagnetic impurity and other symbols have their usual meanings. As indicated in Fig. 5, the cryomagnetic properties of **1** and **2** can be well reproduced by Eq. 2. The best-fit parameters are $g = 2.16$, $J = 7.7 \text{ cm}^{-1}$, $J' = -28.5 \text{ cm}^{-1}$, $\theta = -1.0 \text{ K}$, $N\alpha = 800 \times 10^{-6} \text{ cm}^3 \text{ mol}^{-1}$, and $\rho = 0.017$ for **1** and $g = 2.15$, $J = 7.0 \text{ cm}^{-1}$, $J' = -27.0 \text{ cm}^{-1}$, $\theta = -2.0 \text{ K}$, $N\alpha = 1000 \times 10^{-6} \text{ cm}^3 \text{ mol}^{-1}$, and $\rho = 0.085$ for **2**. The discrepancy factor defined as $R(\chi) = [\sum(\chi_{\text{obsd}} - \chi_{\text{calcd}})^2 / \sum(\chi_{\text{obsd}})^2]^{1/2}$ was 0.042 for **1** and 0.040 for **2**.

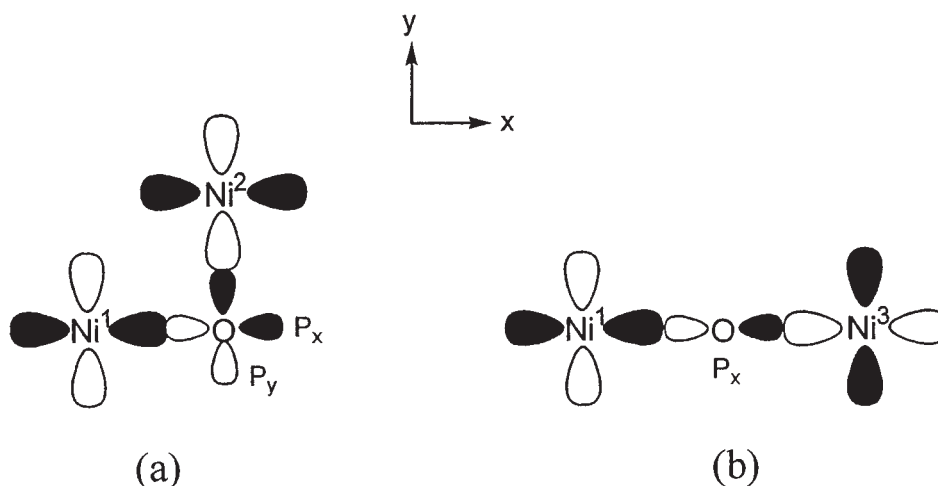


Fig. 7. Spin exchange mechanism (a) between adjacent Ni centers and (b) between diagonal Ni centers.

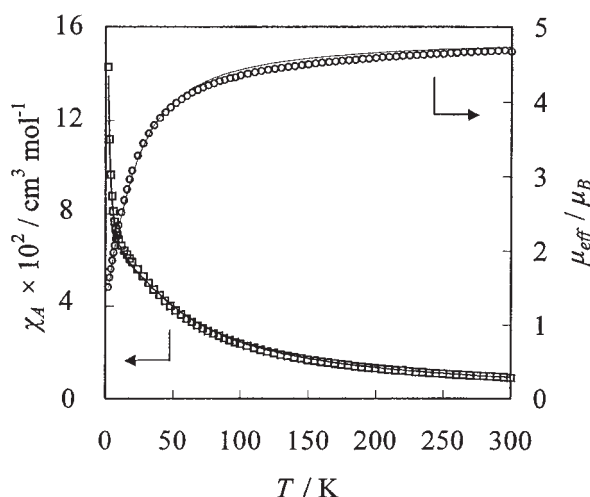


Fig. 8. χ_M vs T and μ_{eff} vs T curves for **3**.

The above magnetic studies indicate that ferromagnetic interaction operates between the adjacent Ni ions and antiferromagnetic interaction operates between the diagonal Ni ions. The ferromagnetic interaction between the adjacent Ni centers can be explained by $d_{x^2-y^2}(\text{Ni}^1) \parallel p_x(\text{O}) \perp p_y(\text{O}) \parallel d_{x^2-y^2}(\text{Ni}^2)$ pathway and the antiferromagnetic interaction between the diagonal Ni centers by $d_{x^2-y^2}(\text{Ni}^1) \parallel p_x(\text{O}) \parallel d_{x^2-y^2}(\text{Ni}^2)$ pathway²¹ (Fig. 7).

The effective magnetic moment of **3** (per Mn) is $4.67 \mu_B$ at room temperature; this moment decreased with decreasing temperature to $1.51 \mu_B$ at 2 K (Fig. 8). Magnetic simulations for **3** were carried out using the magnetic susceptibility expression for the $(S_1 = 2)-(S_2 = 2)$ system:

$$\chi_A = (1 - \rho)\{Ng^2\beta^2/k(T - \theta)\}\{A/B\} + \rho\{4Ng^2\beta^2/kT\} + N\alpha \quad (3)$$

where $A = 30 \exp(20x) + 14 \exp(12x) + 5 \exp(6x) + \exp(2x)$ and $B = 9 \exp(20x) + 7 \exp(12x) + 5 \exp(6x) + 3 \exp(2x) + 1$ with $x = J/kT$.

The cryomagnetic property of **3** can be reproduced by this expression using $J = -2.5 \text{ cm}^{-1}$, $g = 2.0$, $N\alpha = 200 \times 10^{-6} \text{ cm}^3 \text{ mol}^{-1}$, and $\rho = 0.08$. The discrepancy factor for the mag-

netic simulation was 0.067. The result indicates a weak antiferromagnetic interaction between the Mn^{III} ions. It is generally known that the spin exchange in $(\mu\text{-oxo})\text{bis}(\mu\text{-carboxylato})\text{-dimanganese(III)}$ complexes are weakly antiferromagnetic.²²

Conclusion

The macrocyclic ligand derived from the cyclic condensation of four molecules of 3-aminomethyl-5-methylsalicylaldehyde afforded two tetranuclear Ni^{II} complexes, $[\text{Ni}_4(\text{L})(\text{OH})(\text{H}_2\text{O})_4](\text{ClO}_4)_3$ (**1**) and $[\text{Ni}_4(\text{L})(\text{O})(\text{dmf})_4](\text{ClO}_4)_2$ (**2**). Both have a square Ni₄-core with a μ_4 -hydroxo or μ_4 -oxo group at the center of the core. A similar condensation using Mn^{II} in open air afforded $[\text{Mn}_2(\text{H}_2\text{L})(\text{OH})(\text{AcO})_2(\text{H}_2\text{O})]\text{Br}$ (**3**) that has a μ -hydroxo- μ -carboxylato-dimanganese(III) core in the framework of the di-protonated macrocyclic ligand $(\text{H}_2\text{L})^{2-}$. This structure is preferred because a square Mn₄-core with small Mn^{III} does not fit the cavity of L^{4-} . The Ni^{II} complexes show a ferromagnetic interaction between the adjacent Ni^{II} centers and an antiferromagnetic interaction between the diagonal Ni^{II} centers. A weak antiferromagnetic interaction occurs in the dinuclear Mn^{III} complex.

This work was supported by a Grant-in-Aid for Scientific Research Program (No. 13640561) from the Ministry of Education, Culture, Sports, Science and Technology. One of the authors (M. Ohba) thanks Precursory Research for Embryonic Science and Technology (PRESTO), JST for a financial support.

References

- 1 a) M. Bell, A. J. Edwards, B. F. Hoskins, E. H. Kachab, and R. Robson, *J. Chem. Soc., Chem. Commun.*, **1987**, 1852. b) M. Bell, A. J. Edwards, B. F. Hoskins, E. H. Kachab, and R. Robson, *J. Am. Chem. Soc.*, **111**, 3603 (1989). c) A. J. Edwards, B. F. Hoskins, E. H. Kachab, A. Markiewicz, K. S. Murray, and R. Robson, *Inorg. Chem.*, **31**, 3584 (1992).
- 2 B. F. Hoskins, R. Robson, and P. J. Smith, *J. Chem. Soc., Chem. Commun.*, **1990**, 488.
- 3 a) V. McKee and S. S. Tandon, *J. Chem. Soc., Chem. Commun.*, **1988**, 1334. b) V. McKee and S. S. Tandon, *J. Chem. Soc., Chem. Commun.*, **1988**, 1334. c) J. McCrea, V. McKee, T.

- Metcalfe, S. S. Tandon, and J. Wikaira, *Inorg. Chim. Acta*, **297**, 220 (2000).
- 4 V. McKee and S. S. Tandon, *J. Chem. Soc., Dalton Trans.*, **1991**, 221.
- 5 V. McKee and S. S. Tandon, *Inorg. Chem.*, **28**, 2902 (1989).
- 6 S. S. Tandon, L. K. Thompson, and J. N. Beidson, *J. Chem. Soc., Chem. Commun.*, **1992**, 911.
- 7 M. Yonemura, H. Ōkawa, M. Ohba, D. E. Fenton, and L. K. Thompson, *Chem. Commun.*, **2000**, 817.
- 8 Y. Nakamura, M. Yonemura, K. Aratake, N. Usuki, M. Ohba, and H. Ōkawa, *Inorg. Chem.*, **40**, 3739 (2001).
- 9 A. Hori, M. Yonemura, M. Ohba, and H. Ōkawa, *Bull. Chem. Soc. Jpn.*, **74**, 495 (2001).
- 10 D. T. Cromer and J. T. Waber, "International Tables for X-ray Crystallography, Vol. IV," The Kynoch Press, Birmingham, England (1974).
- 11 D. C. Creagh and W. J. McAuley, "International Tables for Crystallography, Vol. C," Kluwer Academic Publishers, Boston (1992), pp. 219–222.
- 12 D. C. Creagh and W. J. McAuley, "International Tables for Crystallography, Vol. C," Kluwer Academic Publishers, Boston (1992), pp. 200–206.
- 13 teXsan, Crystal Structure Analysis Package, Molecular Structure Corporation, Houston, TX, 1985 and 1999.
- 14 B. Bosnich, *J. Am. Chem. Soc.*, **90**, 627 (1968).
- 15 R. S. Dowing and F. L. Urbach, *J. Am. Chem. Soc.*, **91**, 5977 (1969).
- 16 G. B. Deacon and R. J. Phillips, *Coord. Chem. Rev.*, **33**, 227 (1980).
- 17 C. K. Johnson, Report 3794, Oak Ridge National Laboratory, Oak Ridge, TN (1965).
- 18 Crystallographic data for **3**: $a = 11.756(7)$ Å, $b = 19.188(11)$ Å, $c = 20.723(12)$ Å, $\beta = 96.667(9)$, $V = 4643.016(1)$ Å³, crystal system = monoclinic, space group = $P2_1/c$, $R1 = 0.1236$ ($I > 2\sigma(I)$, 3715 obsd).
- 19 R. D. Shannon and C. T. Prewitt, *Acta Crystallogr.*, **B25**, 925 (1969).
- 20 R. Hotzelmann, K. Wieghardt, J. Ensling, H. Romstedt, P. Gütlich, E. Bill, U. Flörke, and H.-J. Haupt, *J. Am. Chem. Soc.*, **114**, 9470 (1992), and references therein.
- 21 A. P. Ginsberg, *Inorg. Chim. Acta*, **5**, 45 (1971).
- 22 B. Holzelmann, K. Wieghardt, U. Flörke, H.-J. Haupt, D. C. Weatherburn, J. Bonvoisin, G. Blondin, and J.-J. Girerd, *J. Am. Chem. Soc.*, **114**, 1681 (1992).